

# Floorplan-SLAM: A Real-Time, High-Accuracy, and Long-Term Multi-Session Point-Plane SLAM for Efficient Floorplan Reconstruction

Haolin Wang<sup>1,2,†</sup>, Zeren Lv<sup>3,†</sup>, Hao Wei<sup>1,\*</sup>, Haijiang Zhu<sup>3</sup> and Yihong Wu<sup>1,2,\*</sup>

**Abstract**—Floorplan reconstruction provides structural priors essential for reliable indoor robot navigation and high-level scene understanding. However, existing approaches either require time-consuming offline processing with a complete map, or rely on expensive sensors and substantial computational resources. To address the problems, we propose Floorplan-SLAM, which incorporates floorplan reconstruction tightly into a multi-session SLAM system by seamlessly interacting with plane extraction, pose estimation, and back-end optimization, achieving real-time, high-accuracy, and long-term floorplan reconstruction using only a stereo camera. Specifically, we present a robust plane extraction algorithm that operates in a compact plane parameter space and leverages spatially complementary features to accurately detect planar structures, even in weakly textured scenes. Furthermore, we propose a floorplan reconstruction module tightly coupled with the SLAM system, which uses continuously optimized plane landmarks and poses to formulate and solve a novel optimization problem, thereby enabling real-time incremental floorplan reconstruction. Note that by leveraging the map merging capability of multi-session SLAM, our method supports long-term floorplan reconstruction across multiple sessions without redundant data collection. Experiments on the VECToR and the self-collected datasets indicate that Floorplan-SLAM significantly outperforms state-of-the-art methods in terms of plane extraction robustness, pose estimation accuracy, and floorplan reconstruction fidelity and speed, achieving real-time performance at 25–45 FPS without GPU acceleration, which reduces the floorplan reconstruction time for a  $1000\text{ m}^2$  scene from over 10 hours to just 9.44 minutes.

## I. INTRODUCTION

Indoor robot navigation and high-level scene understanding have become critical components in a variety of applications, ranging from service robots in assisted living environments to autonomous drones operating in complex indoor facilities. In these scenarios, generating a floorplan in real-time is particularly advantageous, as it not only provides geometric structure for accurate localization but also furnishes semantic cues for higher-level decision-making.

\*This work was supported by the National Natural Science Foundation of China under Grand No. 62402493 and the Youth Program of State Key Laboratory of Multimodal Artificial Intelligence Systems under Grand No. MAIS2024215. (Corresponding authors: Hao Wei and Yihong Wu.)

<sup>1,2</sup>Haolin Wang, Hao Wei and Yihong Wu are with the State Key Laboratory of Multimodal Artificial Intelligence Systems, Institute of Automation, Chinese Academy of Sciences, Beijing 100190, China. Haolin Wang and Yihong Wu are also with the School of Artificial Intelligence, University of Chinese Academy of Sciences, Beijing 100190, China (e-mail: {wanghaolin2023; weihao2019; yihong.wu}@ia.ac.cn).

<sup>3</sup>Zeren Lv and Haijiang Zhu are with the College of Information Science and Technology, Beijing University of Chemical Technology, Beijing 100029, China (e-mail: 2022210463@buct.edu.cn, zhuhj@mail.buct.edu.cn).

<sup>†</sup>Haolin Wang and Zeren Lv contributed equally to this work.

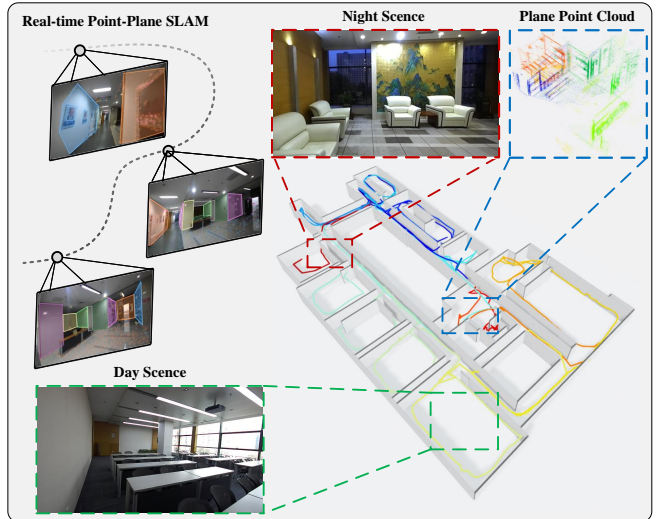


Fig. 1. The real-time floorplan reconstruction results of Floorplan-SLAM on the meeting room sequence from the self-collected dataset. The scene captured over a two-day period consists of low-texture corridors and multiple rooms with many clutter objects.

Despite the growing need for real-time floorplan reconstruction, existing approaches often present significant limitations. Some methods operate in an offline manner, requiring a complete map of the environment prior to reconstruction [1]–[3]. Others rely on expensive sensors such as LiDAR or RGB-D cameras [4], [5], or computationally intensive neural networks [6]–[8], which increase both deployment costs and system complexity.

While monocular or stereo camera-based SLAM has attempted to use high-level features such as planes for real-time vectorized map construction [9]–[11], these methods lack high-level scene layout understanding, thereby failing to achieve complete and compact indoor vectorized reconstruction. Additionally, they cannot perform robust plane extraction in weakly textured scenes.

In this context, an effective real-time solution that works with more accessible and cost-effective sensors, such as stereo cameras, remains uncertain. In this work, we present Floorplan-SLAM, a novel framework that tightly integrates floorplan reconstruction into a SLAM system by seamlessly interacting with plane extraction, pose estimation, and back-end optimization. Unlike prior methods, our approach operates exclusively with stereo cameras under standard computing resources, allowing real-time performance in large-scale indoor settings. A robust plane extraction algorithm is

first developed to handle weakly textured surfaces by leveraging two spatially complementary features in a compact plane parameter space. We further introduce a vectorized reconstruction module tightly integrated with the SLAM system that formulates and solves an innovative optimization problem using the continuously optimized plane landmarks and poses from the SLAM system, enabling real-time incremental floorplan reconstruction. Furthermore, by leveraging the map merging capability of multi-session SLAM, our method supports long-term floorplan reconstruction across multiple sessions without redundant data collection, making it more efficient for large-scale environments.

The contributions of our work can be summarized as follows:

- 1) We propose a robust plane extraction algorithm that operates in a compact plane parameter space and leverages two spatially complementary features to accurately and completely detect planar structures, even in weakly textured scenes.
- 2) We introduce a floorplan reconstruction module that is tightly coupled with the multi-session SLAM system, leveraging continuously optimized plane landmarks and poses from the SLAM system to formulate and solve a binary linear programming problem with novel trajectory constraint thereby enabling real-time, high-accuracy, and long-term floorplan reconstruction.
- 3) Experiments on the VECtor and our self-collected datasets demonstrate that Floorplan-SLAM significantly outperforms state-of-the-art methods in terms of plane extraction robustness, pose estimation accuracy, and floorplan reconstruction fidelity and speed, achieving real-time performance at 25–45 FPS without GPU acceleration.

## II. RELATED WORK

Floorplan reconstruction aims to convert raw sensor data into vectorized geometric models. Some primitives-based vectorized reconstruction methods [1]–[3] detect planes from the input point cloud and then perform a global optimization to select the optimal subset of candidate planes for vectorized reconstruction. However, these methods usually require a prior global map, such as a dense point cloud or a mesh map of the entire scene, which is difficult to obtain from actual point clouds or reconstructed dense meshes due to noise, outliers, and missing data.

With the development of neural networks, deep learning-based vectorized reconstruction methods have become of interest. These methods [6]–[8] typically first project the input dense point cloud onto a top view to create a 2D density map, and then use neural networks to infer the floorplan of the scene from the projected density map. However, these methods are only applicable to specific scenarios, exhibit limited generalizability, and incur high time cost and computational resource consumption.

To achieve real-time vectorized reconstruction, some works [4], [5], [9] utilized visual SLAM to extract plane features from image sequences, which are then used to create

landmarks for map construction. However, these methods either lack high-level scene layout understanding [9], thereby failing to achieve complete and compact indoor vectorized reconstruction, or integrate the acquired poses and scene structures in a loosely coupled manner [4], [5], leading to poor system robustness due to the inability to perform mutual optimization between pose and scene structure. In addition, these methods can only process one set of consecutive images at a time, making it impossible to merge multiple sequences and achieve long-term mapping.

Furthermore, these methods typically utilize RGB-D [5] or neural networks [4], [9] for plane extraction, which is challenging for stereo cameras. In [11], a plane extraction method based on intersecting lines that satisfy specific geometric constraints was proposed. However, this method cannot accurately distinguish real planes from pseudo-planes and is highly susceptible to noise. To enhance the robustness of plane extraction, a region-growing-based plane extraction method was introduced in [10]. Nevertheless, it struggles to extract complete planes in weakly textured scenes and does not fully leverage visual information.

## III. POINT-PLANE-BASED STEREO SLAM SYSTEM

To transform and integrate the planar structure obtained from each frame into the global map, the camera pose of each frame needs to be estimated. Therefore, we propose a point-plane-based stereo SLAM system to estimate camera poses, while creating and managing plane landmarks, which are further processed for floorplan reconstruction in Section IV. The proposed SLAM system utilizes point and plane features, as well as planar regularities, to estimate the camera pose. We refer the reader to [10] for more details on the pose estimation. Next, we focus on describing the operations related to plane landmark management and multi-session map merging.

### A. Plane Extraction

1) *Support Point Extraction*: We employ both the Sobel and ORB features for plane extraction, based on the insight that these two types of features focus on distinct yet complementary regions of a plane: Sobel predominantly captures boundary edges, while ORB detects interior corner points. By harnessing their complementary strengths, we achieve more robust and comprehensive plane extraction. Specifically, we first rectify the input stereo pair, ensuring that stereo correspondences are restricted to the same row in both images. Next, we perform ORB and Sobel feature matching across the stereo images to establish a set of correspondences, followed by consistency checks and outlier removal, thus obtaining a collection of 2D support points. For a 2D support point with pixel coordinates  $(u, v)$  and disparity value  $d$ , its 3D coordinates  $\mathbf{p}_s$  are computed through triangulation as follows:

$$\mathbf{p}_s = [x \ y \ z]^\top = \left[ \frac{(u-c_x)z}{f_x} \quad \frac{(v-c_y)z}{f_y} \quad \frac{f_x b}{d} \right]^\top, \quad (1)$$

where  $(f_x, f_y)$  is the focal length,  $(c_x, c_y)$  is the principal point, and  $b$  is the baseline, all known from calibration.

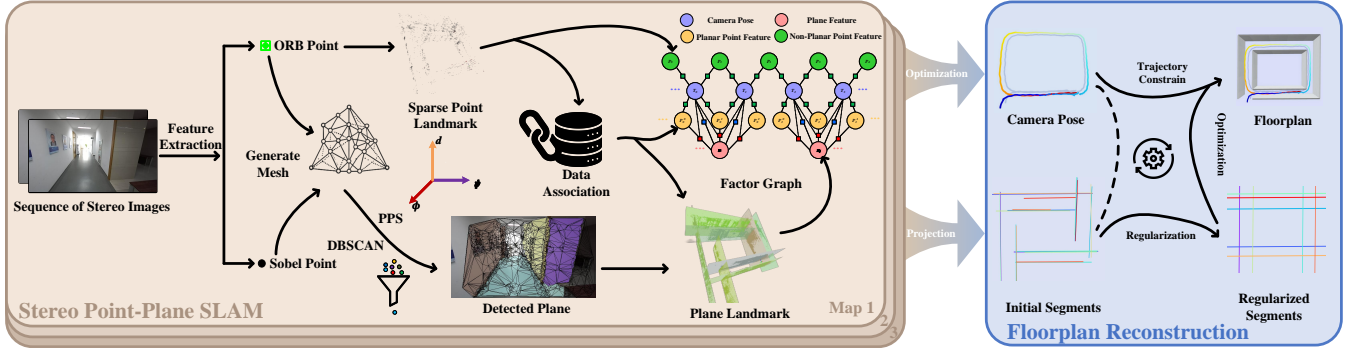


Fig. 2. System Overview. The proposed system consists of two stages: Stereo Point-Plane SLAM and Floorplan Reconstruction. The latter utilizes optimized plane landmarks and trajectory information to generate an accurate and well-structured floorplan.

2) *Mesh Generation*: Because the support points acquired through stereo matching are relatively sparse, the estimated normal vectors of these points exhibit significant errors, rendering them unsuitable as reliable information for plane extraction. Therefore, we employ a set of triangles obtained via Delaunay triangulation [12] on the 2D support points, with these support points serving as vertices, as the fundamental units for plane extraction. Then, we project these triangles into 3D space using the 3D coordinates of the support points to obtain a 3D mesh. We further prune the mesh by discarding triangles in the 3D mesh with long edges, high aspect ratios, and small acute angles [13].

3) *Plane Parameter Space Construction*: Each triangle in the 3D mesh is considered a planar patch, represented by  $\pi = [\mathbf{n}^\top, d]^\top$  in Cartesian space, where  $\mathbf{n} = [n_x, n_y, n_z]^\top$  is the unit normal vector calculated by the cross product of two triangle edges, and  $d$  is the distance from the origin to this triangle planar patch. We project these triangle planar patches from Cartesian space into Plane Parameter Space (PPS) [14], which compactly represents planes in Cartesian space. Specifically, given a triangle planar patch in Cartesian space, its representation in the PPS is a point  $\mathbf{p}_\pi$ :

$$\mathbf{p}_\pi = \begin{bmatrix} \phi \\ \psi \\ d \end{bmatrix} = \begin{bmatrix} \text{atan2}(n_y, n_x) \\ \arccos(n_z) \\ d \end{bmatrix}, \quad (2)$$

where  $\phi$  and  $\psi$  are the azimuth and elevation angles of the normal vector respectively.

4) *Plane Parameters Estimation*: Ideally, the coplanar triangle planar patches in Cartesian space share the same coordinates in the PPS. However, due to noise, the coordinates of these coplanar triangle planar patches in the PPS are not exactly the same but rather close. Therefore, the problem of detecting coplanar triangle planar patches in Cartesian space is transformed into a point clustering problem in the PPS. We employ DBSCAN [15] to cluster the points in the PPS, which is robust to noise.

After obtaining the coplanar triangle planar patches, the vertices of these triangles are coplanar points. We apply RANSAC [16] to these coplanar points to obtain accurate plane parameters, and only planes with an inlier ratio exceeding  $\theta_i$  are added to the plane feature set. In our experiments,

$\theta_i$  is set to 0.75.

### B. Plane Landmark Management

For any two plane landmarks  $\Pi_i$  and  $\Pi_j$ , if the angle between their normal vectors is less than  $\theta_c$  and the minimum point-to-plane distances from the support points of  $\Pi_i$  to  $\Pi_j$  and from  $\Pi_j$  to  $\Pi_i$  are both less than  $d_c$ , we remove the plane landmark with fewer keyframe observations and transfer its observation information and support points to another plane landmark, followed by RANSAC to update the plane points. The above operations continue throughout the entire process of the system. In our experiments,  $d_a$  is set to 1 cm,  $\theta_c$  is set to 5°, and  $d_c$  is set to 2 cm.

### C. Multi-Session Map Merging

We use DBoW2 [17] for place recognition and compute the aligning transformation  $\mathbf{T}_{cm}$  between the two maps. Then, a local window is defined, comprising matching keyframes from both maps, their respective neighbors in the covisibility graph, and the observed point and plane landmarks. Duplicated landmarks from the current map are removed within this local window, and their observations are transferred to the corresponding landmarks in the matching map. A local bundle adjustment (BA) is performed to optimize all keyframes and the point and plane landmarks they observe within the local window. Pose graph optimization is then conducted on the essential graph of the merged map, with the keyframes in the local window fixed. Finally, a global BA is executed in a separate thread to further optimize the merged map and enhance overall consistency. By merging sequences captured at different times, we do not need to capture all map areas in a single pass, which is crucial for large-scale scene long-term mapping, as it significantly reduces the computational and storage burden on the acquisition devices. Notably, during each BA process, the parameters of plane landmark  $\Pi_k$  are optimized, and its support points are updated by aggregating the support points of its observations  $\pi_{i,k}$  in the keyframes into  $\Pi_k$  followed by RANSAC, thereby providing a more accurate scene layout for the subsequent floorplan reconstruction.

## IV. FLOORPLAN RECONSTRUCTION

### A. Candidate Wall Segment Generation

We first select valid plane landmarks that are approximately perpendicular to the ground. We then project their plane points onto the ground to obtain projection lines and support points, thereby generating 2D wall segments. We further merge segments whose angle is less than  $\theta_r$  and share more than  $n_r$  support points sufficiently close to both segments, in order to improve the regularity of the wall segments. Next, we extend and pairwise intersect these segments to generate candidate wall segments. In our experiments,  $\theta_r$  is set to  $10^\circ$ , and  $n_r = \min(|\text{SP}(s_i)|, |\text{SP}(s_j)|)/10$ , where  $|\text{SP}(s_i)|$  represents the number of support points of  $s_i$ .

### B. Wall Segment Selection

Given a set of candidate wall segments  $C = \{c_1, c_2, \dots, c_N\}$  introduced by the pairwise intersection process, we aim to select an optimal subset of this set through global optimization, thereby achieving accurate floorplan reconstruction. We formulate the optimization problem as a binary linear programming problem under hard constraints and solve it via an energy minimization approach. The objective function of this optimization problem consists of three energy terms, the point fitting term  $E_f$ , the point coverage term  $E_c$ , and the model complexity term  $E_m$ , subject to multiple hard constraints.

1) *Point Fitting Term*: This term aims to evaluate the fitting degree between candidate wall segments and their support point sets:

$$E_f = 1 - \frac{1}{|P|} \sum_{i=1}^N f(c_i) x_i, \quad (3)$$

$$f(c) = \sum_{p \in \text{SP}(c) | \text{dist}(p, c) < \varepsilon_f} \left( 1 - \frac{\text{dist}(p, c)}{\varepsilon_f} \right), \quad (4)$$

where  $|P|$  is the total number of support points of candidate wall segments,  $\text{SP}(c)$  is the support point set of segment  $c$ , and  $\text{dist}(p, c)$  is the distance from point  $p$  to segment  $c$ . Only points with a distance less than  $\varepsilon_f$  to the corresponding segment are used in the calculation of  $f(c)$ , and  $\varepsilon_f$  is set to the average distance between candidate wall segments and their support point sets in our experiment.

2) *Point Coverage Term*: This term aims to appropriately evaluate the coverage degree between candidate wall segments and their support point sets in cases where the point cloud is incomplete due to missing data. We consider a segment to be covered by two adjacent support points if the distance between these points is less than  $\varepsilon_c$ :

$$E_c = \frac{1}{N} \sum_{i=1}^N \left( 1 - \frac{\text{len}_{\text{cov}}(c_i)}{\text{len}(c_i)} \right) x_i, \quad (5)$$

where  $\text{len}_{\text{cov}}(c_i)$  is the total length of the portion of  $c_i$  covered by its support points, and  $\text{len}(c_i)$  is the length of  $c_i$ . In our experiments,  $\varepsilon_c = 10 \cdot \text{density}(P)$ , where  $\text{density}(P)$  represents the average of the mean distances between all support points and their respective 10-nearest neighbors.

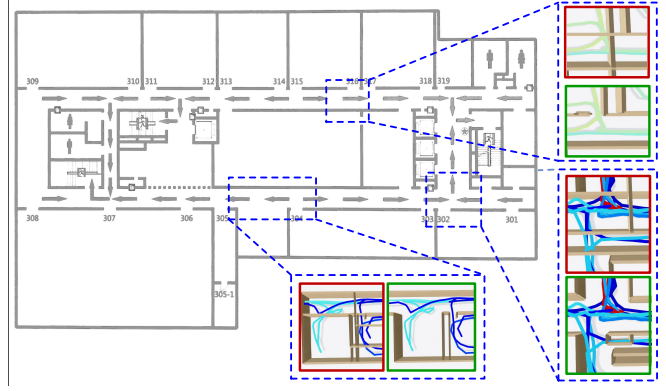


Fig. 3. Comparison of floorplan reconstruction results with and without trajectory constraints. The top-left shows the CAD floor plans provided by the meeting room scenario in the self-collected dataset. The red box indicates the reconstruction results without trajectory constraints, while the green box represents the reconstruction results with trajectory constraints. The trajectory constraints ensure that the reconstructed floorplan contains navigable openings, thereby significantly improving reconstruction accuracy.

3) *Model Complexity Term*: This term aims to evaluate the complexity of the reconstructed floorplan and maintain it at an appropriate level of complexity. Specifically, if an intersection point  $v_i$  generated by pairwise intersection of the wall segments is connected by non-collinear candidate wall segments  $c_i$  and  $c_j$ , and both  $c_i$  and  $c_j$  are selected, we consider  $v_i$  to introduce a sharp structure:

$$E_m = \frac{1}{M} \sum_{i=1}^M \mathbb{I}_{\text{sharp}}(v_i), \quad (6)$$

where  $\mathbb{I}_{\text{sharp}}(v_i)$  is an indicator function that equals 1 if  $v_i$  introduces a sharp structure, and 0 otherwise.

4) *Constraints*: Trajectory information is a unique component of the SLAM system, as it inherently contains prior knowledge about navigable areas, as shown in Fig. 3. We exclude candidate wall segments that are crossed by the trajectory from the selection:

$$\sum_{i=1}^N \mathbb{I}_{\text{cross}}(c_i) \cdot x_i = 0, \quad (7)$$

where  $\mathbb{I}_{\text{cross}}(c_i)$  is an indicator function that equals 1 if  $c_i$  is crossed by the trajectory, and 0 otherwise. To ensure that the floorplan is closed except at the passable areas, the intersection point  $v_i$ , which is not connected by segments crossed by the trajectory, must be connected by at least two and at most four candidate wall segments. Otherwise, it must be connected by at least one and at most  $4 - n_c$  candidate wall segments:

$$\begin{cases} \sum_{i=1}^N x_i \in \{0, 2, 3, 4\}, & \text{if } \forall c_i \in \mathcal{C}(v_j), \mathbb{I}(c_i) = 0, \\ 0 \leq \sum_{i=1}^N x_i \leq 4 - n_c, & \text{if } \exists c_i \in \mathcal{C}(v_j), \mathbb{I}(c_i) = 1, \end{cases} \quad (8)$$

where  $\mathcal{C}(v_j)$  and  $n_c$  represent the set of candidate wall segments connected to  $v_j$  and the number of segments in the set that are traversed by the trajectory, respectively.

5) *Optimization*: The objective function  $E$  of this optimization problem is the weighted sum of the above energy terms:

$$E = \lambda_f E_f + \lambda_c E_c + \lambda_m E_m. \quad (9)$$

We utilize the SCIP solver [18] to minimize (9) subject to the hard constraints (7) and (8) to obtain the optimal subset of candidate wall segments. Then, the floorplan is reconstructed by assembling the segments in the optimal subset.

## V. EXPERIMENT

### A. Plane Extraction Performance Evaluation

Since we utilize the extracted planes for floorplan reconstruction, the accuracy and stability of these planes are crucial to the overall quality of the reconstruction outcomes. We evaluate our plane extraction algorithm and compare it with the plane extraction modules of two point-plane-based stereo SLAM systems, Stereo-Plane-SLAM [11] and RSS [10]. We use plane reprojection error and plane observation count as evaluation metrics to measure the accuracy and stability of the extracted planes, respectively. Specifically, the plane reprojection error represents the matching error between plane observations and landmarks, while the plane observation count indicates the average number of times each valid plane landmark is observed by keyframes. To eliminate the impact of trajectory errors on plane extraction performance, we utilize ground-truth trajectories for evaluation.

Table I compares the plane extraction performance of different methods on the VECtor and self-collected datasets. Our method significantly outperforms SP-SLAM and RSS in both accuracy and stability. Because RSS uses a region-growing strategy for plane extraction, insufficient support points in weakly textured regions can lead to multiple planes being extracted from a single surface, making them more prone to noise and thus less stable. In contrast, our method employs DBSCAN clustering in the PPS space to robustly detect complete and accurate discontinuous planes even in weakly textured scenes lacking support points. Additionally, by using both ORB and Sobel features, which focus on corner and edge regions respectively, our method can extract more planes than RSS, which relies solely on Sobel features, particularly in VECtor scenarios with numerous patches on ceilings and floors, as illustrated in Fig. 4. SP-SLAM relies on intersecting lines for plane extraction. Although many line segments can be identified, strict filtering to avoid spurious planes leaves only a few that contribute to plane extraction. Moreover, these segments are highly sensitive to noise, making the extracted planes unstable across multiple frames and reducing their overall accuracy and stability.

### B. Localization Accuracy Evaluation

Accurate poses allow planes extracted from different frames to be seamlessly integrated into the global map, maintaining the global consistency of the incrementally reconstructed floorplan. We evaluate the localization performance

TABLE I  
PLANE EXTRACTION PERFORMANCE COMPARISON ON THE VECTOR  
AND SELF-COLLECTED DATASETS

Sequence	Reprojection Error ↓			Observation Count ↑		
	SP <sup>1</sup>	RSS	Ours	SP <sup>1</sup>	RSS	Ours
corridors	0.033	0.028	<b>0.009</b>	11.909	32.059	<b>103.727</b>
school	0.039	0.029	<b>0.011</b>	6.250	28.265	<b>79.375</b>
meeting rooms	0.048	0.017	<b>0.007</b>	15.333	34.867	<b>226.286</b>
offices	0.062	0.022	<b>0.008</b>	19.750	22.528	<b>135.167</b>
café	0.057	0.024	<b>0.008</b>	14.333	20.286	<b>147.250</b>

<sup>1</sup> SP is the abbreviation for Stereo-Plane-SLAM [11].



Fig. 4. Comparison of plane extraction results on the VECtor (upper) and self-collected (lower) datasets. ORB features are represented by crosses, and Sobel features are represented by dots in our method. The plane boundaries in both RSS and our approach are determined by the convex hull of the corresponding plane points.

of our method in large-scale indoor scenes and compare it with the most relevant state-of-the-art visual SLAM systems, including ORB-SLAM3 (stereo mode) [19], Stereo-Plane-SLAM [11], and RSS [10]. To assess the impact of plane features, we also conduct an ablation study using a point-only variant of our system. Experiments are performed on the public VECtor dataset [20] and a self-collected dataset, both containing sequences exceeding 100 meters. The self-collected dataset was captured using a ZED2 camera with GeoSLAM as ground truth (Fig. 5). We align the estimated trajectory with ground truth using the Umeyama algorithm without scaling and use the RMSE of the absolute trajectory error (ATE) to measure global drift. Each sequence is run ten times to mitigate multi-thread randomness, and the median results are reported.

As shown in Table II, our method outperforms ORB-SLAM3 and the Point-Only variant across all sequences, especially on the *units* sequences of the VECtor dataset and the *Basement* sequence of the self-collected dataset, which feature challenging scenes characterized by low texture, dynamically changing illumination, and motion blur. In these scenarios, our approach achieves a notable accuracy improvement of 0.5–0.9 m. This can be attributed to two primary reasons: (1) Compared with point correspondences, plane correspondences are more accurate and stable, particularly in the aforementioned challenging scenarios; (2) Planar structures, especially life-long structures such as walls with extensive spatial coverage, can be tracked across considerable distances, thereby providing comprehensive and



Fig. 5. Our Self-Collected dataset Setup.

TABLE II  
LOCALIZATION PERFORMANCE COMPARISON ON THE  
VECTOR AND SELF-COLLECTED DATASET (ATE  
RMSE [M])

Sequence	ORB <sup>1</sup>	SP <sup>1</sup>	RSS	PO <sup>1</sup>	Ours
corridors_dolly	0.96	0.95	0.94	0.96	<b>0.93</b>
units_dolly	2.48	2.49	1.81	2.42	<b>1.64</b>
units_scooter	1.89	1.82	1.74	1.84	<b>1.41</b>
school_dolly	1.40	1.39	1.40	1.39	<b>1.37</b>
school_scooter	1.39	<b>1.30</b>	1.33	1.38	1.31
Corridor	1.53	1.57	1.38	1.54	<b>1.29</b>
Room	1.40	1.25	1.18	1.38	<b>1.07</b>
Stair	2.35	1.79	1.66	2.40	<b>1.60</b>
Basement	2.49	2.41	1.61	2.52	<b>1.56</b>

<sup>1</sup> ORB, SP, and PO are abbreviations for ORB-SLAM3, Stereo-Plane-SLAM, and the point-only variant of our system, respectively.

reliable constraints for pose estimation. Furthermore, in comparison with the two point-plane-based stereo SLAM systems, our method yields the smallest average RMSE and still demonstrates superior performance on these challenging sequences. This can be attributed to the more comprehensive and accurate plane constraints introduced by our advanced plane extraction method, as demonstrated in Section V-A.

### C. Floorplan Reconstruction Performance Evaluation

We evaluate the floorplan reconstruction performance of our method on the VECtor [1] and a self-collected dataset, comparing it with two state-of-the-art offline floorplan reconstruction methods: VecIM [1] and RoomFormer [6]. The former employs a gravity-aligned point cloud as input, while the latter uses a 2D density map obtained by projecting the point cloud along the gravity axis. In contrast, our method uses only stereo images as input. VecIM and RoomFormer both utilize a dense multi-view stereo (MVS) point cloud reconstructed by COLMAP [21], which takes advantage of more comprehensive global optimization and additional multi-view information. This results in a more accurate point cloud than that generated by our SLAM system, ensuring fairness in the comparison. We uniformly sample 10K points from the reconstructed floorplan and compute the Hausdorff distance between these sampled points and the ground-truth point cloud to evaluate the reconstruction accuracy, using a dense, high-precision LiDAR point cloud as the ground truth.

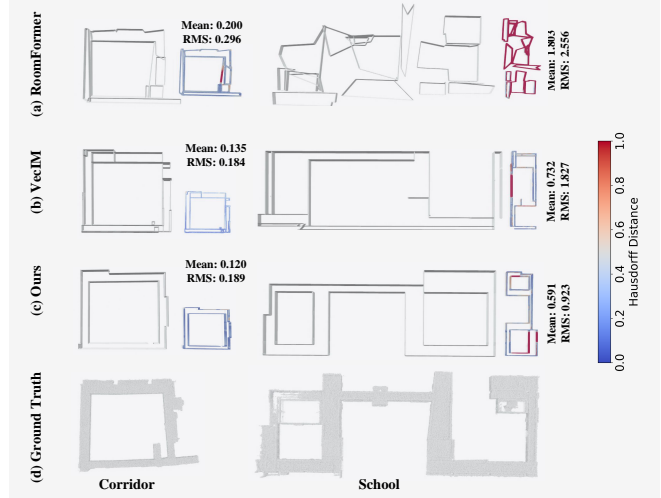


Fig. 6. Floorplan reconstruction results on the VECtor Dataset of RoomFormer, VecIM, and Ours. We compute and visualize the mean (m) and RMS Hausdorff error (m) between the reconstructed models and the LiDAR point cloud. The error distribution is color-coded, where blue indicates smaller errors and red represents larger errors.

1) *Evaluation on the VECtor Dataset:* Figure 6 shows the qualitative and quantitative results on the VECtor dataset, where our method achieves the lowest mean Hausdorff error and reconstructs a more regular floorplan closer to the real scene. Since VecIM directly applies efficient RANSAC to detect planes from the entire point cloud, it is highly susceptible to outliers and noise, which is an inevitable issue for MVS point clouds in weakly textured scenes. As a result, it extracts many incorrect planes, leading to numerous redundant layered structures. Moreover, VecIM enforces the floorplan to be closed, resulting in many erroneous closed regions. In contrast, although our method also faces challenges in weakly textured regions, it leverages plane points from reliable plane landmarks that persist across multiple frames and undergo continuous optimization. While these points are sparser, they are robust matches carefully selected through strict consistency checks and outlier removal, resulting in significantly higher accuracy and structural regularity. Moreover, by incorporating trajectory information, our method correctly handles navigable areas and openings, avoiding erroneous closed regions.

2) *Evaluation on the Self-collected Dataset:* To evaluate the floorplan reconstruction performance of our method in complex indoor environments containing numerous non-lifelong structures (e.g., tables, chairs), and to assess its long-term floorplan reconstruction capability, we used a ZED2 camera to collect data in three large-scale scenes, covering meeting rooms, offices, and a café, among other places, each covering an area of 1000 square meters. In the conference room scenario, due to the inconsistent accessibility of different meeting rooms, we conducted five separate data collections over two days, with each sub-session covering a different region of the scene. The qualitative and quantitative results of floorplan reconstruction on the

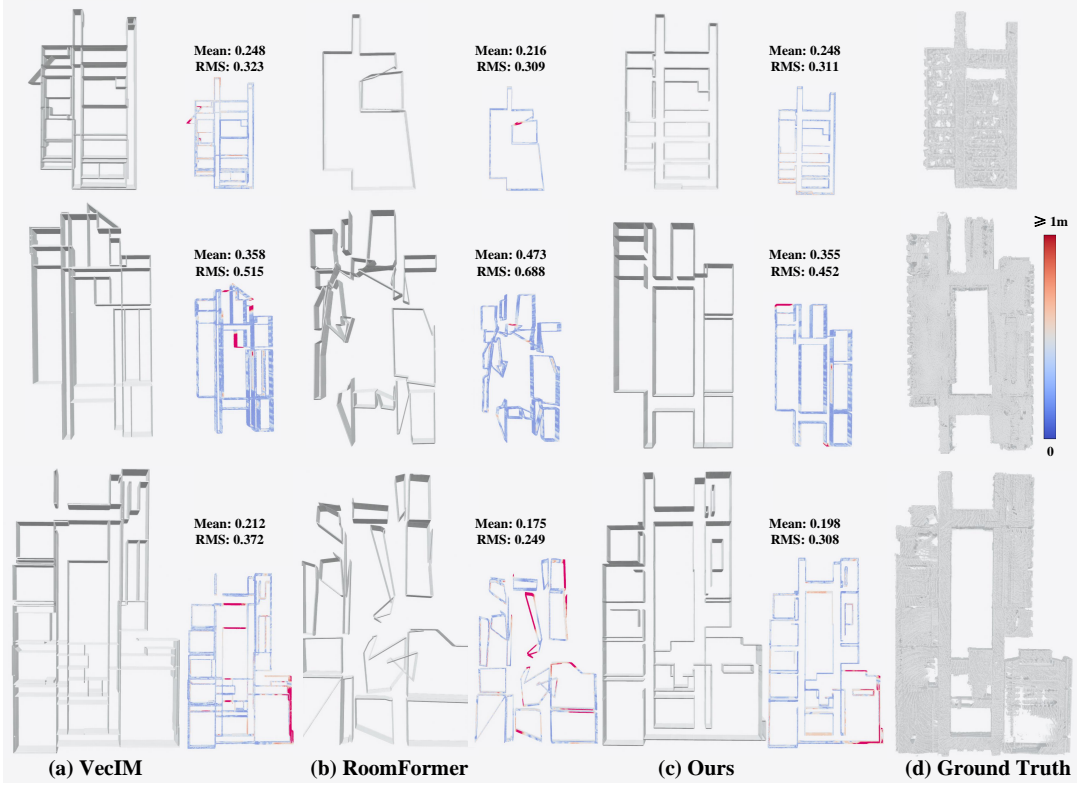


Fig. 7. Floorplan reconstruction results on the self-collected dataset of VecIM, RoomFormer and Ours. For each reconstruction result, the mean Hausdorff error(m) and the error model are computed from the output to the ground truth. From top to bottom, we display the office, café, and meeting rooms, respectively.

self-collected dataset are presented in Fig. 7. Our method still reconstructs the most regular and faithful floorplan. Benefiting from the rich textures, the MVS point cloud exhibits relatively low error, enabling VecIM to accurately reconstruct the main structures of the scene. However, due to the presence of non-lifelong objects, VecIM is unable to focus solely on extracting lifelong structures and detects numerous temporary structures such as table sides. Consequently, the reconstructed floorplan contains many redundant elements and still fails to effectively handle navigable areas. Although our method may also extract planes belonging to non-life-long objects during the plane extraction stage, these planes typically do not persist across multiple frames. Therefore, they are not considered valid plane landmarks for the vectorized reconstruction module, which enables our approach to specifically reconstruct life-long structures. Furthermore, the trajectory information is fully leveraged to handle openings in navigable areas, such as corridors and room entrances, ensuring that the reconstructed floorplan accurately represents passable regions. In addition, although our self-collected dataset contains room scenes, RoomFormer lacks generalizability for large-scale environments and thus can only generate a limited number of correctly identified rooms. Notably, by sequentially merging multiple subsequences, our method yields a complete large-scale floorplan that encompasses multiple meeting rooms, exhibiting remarkable accuracy and regularity, which strongly demon-

TABLE III  
EXECUTION TIME COMPARISON (IN MILLISECONDS).

Set.	Sys.	ORB-SLAM3		Ours	
	Seq.	school 1224×1024	Meeting 640×360	school 1224×1024	Meeting 640×360
Tra.	PE <sup>1</sup>	28.77	13.58	28.96	13.51
	PIE <sup>1</sup>	-	-	29.92	14.01
	PP <sup>1</sup>	8.44	5.54	11.2	8.32
	Total	37.36	19.28	41.38	22.61
Rec.	SG <sup>1</sup>	-	-	42.30	37.37
	SS <sup>1</sup>	-	-	39.32	55.50
	Total	-	-	81.62	92.87

<sup>1</sup> PE, PIE, PP, SG, and SS are the abbreviations for ORB Point Feature Extraction, Plane Feature Extraction, Pose Prediction, Segment Generation, and Segment Selection, respectively.

strates the long-term globally consistent mapping capability of our approach. As a result, there is no need to acquire the complete scene data in a single pass, greatly reducing the complexity of data collection and reconstruction.

#### D. Runtime Analysis

We evaluated the runtime performance of our method on the school sequence from the VECtor dataset and on the Meeting Rooms sequence from our self-collected dataset, comparing the results with ORB-SLAM3. As shown in Table III, we present the runtime of the two threads where our method and ORB-SLAM3 exhibit the most significant differences, while the execution times for the remaining

TABLE IV  
RUNTIME OF EACH MODULE IN THE PROPOSED PLANE  
EXTRACTION ALGORITHM

Sequence	SFE <sup>1</sup>	OFE <sup>1</sup>	MG <sup>1</sup>	DC <sup>1</sup>	PPE <sup>1</sup>	Total
school	20.68	28.96	0.35	0.37	0.24	29.92
Meeting	9.43	13.51	0.19	0.18	0.13	14.01

<sup>1</sup> SFE, OFE, MG, DC, and PPE are the abbreviations for Sobel Feature Extraction, ORB Feature Extraction, Mesh Generation, DBSCAN Clustering, and Plane Parameter Estimation, respectively.

threads are comparable. We utilize parallel CPU threads to independently extract Sobel features and ORB features. Since the former consumes less time, the total plane extraction time is computed as the sum of the ORB feature extraction time and the subsequent plane extraction operations. As shown in Table IV, the runtime of each plane extraction module indicates that ORB feature extraction is the primary time-consuming module. Consequently, our overall plane extraction time is close to that of ORB feature extraction. The floorplan reconstruction module runs on a dedicated thread that operates in parallel with the tracking, local mapping, and loop & map merging threads. It comprises two primary components: segment generation and segment selection. We evaluate the runtime by measuring the duration of the final reconstruction in each sequence, which yields the largest number of segments to be selected and thus represents the most time-consuming execution. Notably, the module leverages plane points provided by valid plane landmarks for floorplan reconstruction, which are typically updated every several frames. As a result, we perform floorplan reconstruction every five frames. This update frequency is sufficient to provide timely updates to the floorplan, thereby enabling real-time floorplan reconstruction.

## VI. CONCLUSION

This paper presents Floorplan-SLAM, a novel approach for real-time, high-accuracy, and long-term floorplan reconstruction, significantly reducing reconstruction time while maintaining superior accuracy and robustness. The proposed method consistently outperformed state-of-the-art approaches in three key aspects: plane extraction robustness, pose estimation accuracy, and floorplan reconstruction fidelity and speed. Experimental results on the VECtor dataset and our self-collected dataset demonstrate the effectiveness of Floorplan-SLAM. Specifically, our algorithm is able to reconstruct a 1000  $m^2$  floorplan in just 9.44 minutes, compared with the over 16 hours and 44 minutes required by the existing offline method [1], achieving a speedup of two orders of magnitude, while yielding more accurate and structured reconstruction results. The real-time performance, achieving 25–45 FPS without GPU acceleration, further underscores the efficiency and practicality of our approach for large-scale indoor floorplan reconstruction. Future work will focus on deeply integrating the floorplan with the SLAM system to fully leverage the high-level scene understanding it

provides, thereby enabling hierarchical localization and map merging in challenging scenarios.

## REFERENCES

- [1] J. Han, M. Rong, H. Jiang, H. Liu, and S. Shen, “Vectorized indoor surface reconstruction from 3d point cloud with multistep 2d optimization,” *ISPRS Journal of Photogrammetry and Remote Sensing*, vol. 177, pp. 57–74, 2021.
- [2] L. Nan and P. Wonka, “Polyfit: Polygonal surface reconstruction from point clouds,” in *Proceedings of the IEEE International Conference on Computer Vision*, 2017, pp. 2353–2361.
- [3] J.-P. Bauchet and F. Lafarge, “Kinetic shape reconstruction,” *ACM Transactions on Graphics (TOG)*, vol. 39, no. 5, pp. 1–14, 2020.
- [4] B. Solarte, Y.-C. Liu, C.-H. Wu, Y.-H. Tsai, and M. Sun, “360-dfpe: Leveraging monocular 360-layouts for direct floor plan estimation,” *IEEE Robotics and Automation Letters*, vol. 7, no. 3, pp. 6503–6510, 2022.
- [5] J.-L. Matez-Bandera, J. Monroy, and J. Gonzalez-Jimenez, “Sigmafp: Robot mapping of 3d floor plans with an rgb-d camera under uncertainty,” *IEEE Robotics and Automation Letters*, vol. 7, no. 4, pp. 12539–12546, 2022.
- [6] Y. Yue, T. Kontogianni, K. Schindler, and F. Engelmann, “Connecting the dots: Floorplan reconstruction using two-level queries,” in *Proceedings of the IEEE/CVF Conference on Computer Vision and Pattern Recognition*, 2023, pp. 845–854.
- [7] S. Stekovic, M. Rad, F. Fraundorfer, and V. Lepetit, “Montefloor: Extending mcts for reconstructing accurate large-scale floor plans,” in *Proceedings of the IEEE/CVF International Conference on Computer Vision*, 2021, pp. 16034–16043.
- [8] J. Chen, C. Liu, J. Wu, and Y. Furukawa, “Floor-sp: Inverse cad for floorplans by sequential room-wise shortest path,” in *Proceedings of the IEEE/CVF International Conference on Computer Vision*, 2019, pp. 2661–2670.
- [9] S. Yang and S. Scherer, “Monocular object and plane slam in structured environments,” *IEEE Robotics and Automation Letters*, vol. 4, no. 4, pp. 3145–3152, 2019.
- [10] H. Wang, H. Wei, Z. Xu, Z. Lv, P. Zhang, N. An, F. Tang, and Y. Wu, “Rss: Robust stereo slam with novel extraction and full exploitation of plane features,” *IEEE Robotics and Automation Letters*, 2024.
- [11] X. Zhang, W. Wang, X. Qi, and Z. Liao, “Stereo plane slam based on intersecting lines,” in *2021 IEEE/RSJ International Conference on Intelligent Robots and Systems (IROS)*. IEEE, 2021, pp. 6566–6572.
- [12] L. P. Chew, “Constrained delaunay triangulations,” in *Proceedings of the third annual symposium on Computational geometry*, 1987, pp. 215–222.
- [13] A. Rosinol, “Densifying sparse vio: a mesh-based approach using structural regularities,” Master’s thesis, ETH Zurich; Massachusetts Institute of Technology, 2018.
- [14] Q. Sun, J. Yuan, X. Zhang, and F. Sun, “Rgb-d slam in indoor environments with sting-based plane feature extraction,” *IEEE/ASME Transactions on Mechatronics*, vol. 23, no. 3, pp. 1071–1082, 2017.
- [15] M. Ester, H.-P. Kriegel, J. Sander, X. Xu *et al.*, “A density-based algorithm for discovering clusters in large spatial databases with noise,” in *kdd*, vol. 96, no. 34, 1996, pp. 226–231.
- [16] M. A. Fischler and R. C. Bolles, “Random sample consensus: a paradigm for model fitting with applications to image analysis and automated cartography,” *Communications of the ACM*, vol. 24, no. 6, pp. 381–395, 1981.
- [17] D. Gálvez-López and J. D. Tardos, “Bags of binary words for fast place recognition in image sequences,” *IEEE Transactions on robotics*, vol. 28, no. 5, pp. 1188–1197, 2012.
- [18] G. Gamrath, D. Anderson, K. Bestuzheva, W.-K. Chen, L. Eifler, M. Gasse, P. Gemander, A. Gleixner, L. Gottwald, K. Halbig *et al.*, “The scip optimization suite 7.0,” 2020.
- [19] C. Campos, R. Elvira, J. J. G. Rodríguez, J. M. Montiel, and J. D. Tardós, “Orb-slam3: An accurate open-source library for visual, visual-inertial, and multimap slam,” *IEEE Transactions on Robotics*, vol. 37, no. 6, pp. 1874–1890, 2021.
- [20] L. Gao, Y. Liang, J. Yang, S. Wu, C. Wang, J. Chen, and L. Kneip, “Vector: A versatile event-centric benchmark for multi-sensor slam,” *IEEE Robotics and Automation Letters*, vol. 7, no. 3, pp. 8217–8224, 2022.
- [21] J. L. Schonberger and J.-M. Frahm, “Structure-from-motion revisited,” in *Proceedings of the IEEE conference on computer vision and pattern recognition*, 2016, pp. 4104–4113.